

outs are due to time variations (Saturnian substorm ?), although the occurrence of the second dropout ~ 11 hours after the first makes this less likely. Examination of solar wind activity measured by Voyager 2 upstream from Saturn during this period may help in evaluating this possibility.

As indicated in Fig. 6, the electron pitch angle distribution appears to be field-aligned and bidirectional, suggesting that there exist closed field lines (except in the intensity dropout regions) all the way to the magnetopause at a distance of $\sim 20 R_S$ above the plane. Ions, on the other hand, show persistent inward flow (toward Saturn) inside the magnetopause with only weak outflow, indicating a source beyond $40 R_S$ and a probable sink closer to the planet. It is likely that these closed field lines could extend several tens or even hundreds of R_S behind the planet.

In summary, although the magnetic field configuration of Saturn appears relatively simple and dipole-like (18), the particle population reveals many striking features in the low-energy spectra, anisotropies, and compositions on both the dayside and nightside, and these features are remarkably different from those of the corresponding populations at Earth and Jupiter.

S. M. KRIMIGIS

Applied Physics Laboratory,
Johns Hopkins University,
Laurel, Maryland 20810

T. P. ARMSTRONG

Department of Physics, University of
Kansas, Lawrence 66044

W. I. AXFORD

Max-Planck Institute for Aeronomy,
D-3411 Katlenburg-Lindau 3,
West Germany

C. O. BOSTROM

Applied Physics Laboratory,
Johns Hopkins University

G. GLOECKLER

Department of Physics and Astronomy,
University of Maryland,
College Park 20742

E. P. KEATH

Applied Physics Laboratory,
Johns Hopkins University

L. J. LANZEROTTI

Bell Laboratories,
Murray Hill, New Jersey 07974

J. F. CARBARY

Applied Physics Laboratory,
Johns Hopkins University

D. C. HAMILTON

Department of Physics and Astronomy,
University of Maryland

E. C. ROELOF

Applied Physics Laboratory,
Johns Hopkins University

References and Notes

1. S. M. Krimigis, T. P. Armstrong, W. I. Axford, C. O. Bostrom, C. Y. Fan, G. Gloeckler, L. J. Lanzerotti, *Space Sci. Rev.* **21**, 329 (1977).
2. S. M. Krimigis, J. F. Carbary, E. P. Keath, C. O. Bostrom, W. I. Axford, G. Gloeckler, L. J. Lanzerotti, T. P. Armstrong, *J. Geophys. Res.*, in press.
3. J. A. Van Allen, M. F. Thomsen, B. A. Randall, *ibid.* **85**, 5709 (1980).
4. F. B. McDonald, A. W. Scharadt, J. H. Trainor, *ibid.*, p. 5813.
5. N. F. Ness *et al.*, *Science* **212**, 211 (1981).
6. E. C. Roelof, *NASA Spec. Publ. SP-199* (1969).
7. L. A. Frank, B. G. Burek, K. L. Ackerson, J. H. Wolfe, J. D. Mihalov, *J. Geophys. Res.* **85**, 5695 (1980).
8. D. C. Hamilton, G. Gloeckler, S. M. Krimigis, L. J. Lanzerotti, *ibid.*, in press.
9. D. C. Hamilton, G. Gloeckler, S. M. Krimigis, C. O. Bostrom, T. P. Armstrong, W. I. Axford, C. Y. Fan, L. J. Lanzerotti, D. M. Hunten, *Geophys. Res. Lett.* **7**, 813 (1980).
10. A. G. W. Cameron, *Space Sci. Rev.* **15**, 121 (1970).
11. J. A. Van Allen, B. A. Randall, M. F. Thomsen, *J. Geophys. Res.* **85**, 5679 (1980).
12. J. A. Simpson, T. S. Bastian, D. L. Chenette, R. B. McKibbin, K. R. Pyle, *ibid.*, p. 5731.
13. W. Fillius and C. McIlwain, *ibid.*, p. 5803.
14. A. Mogro-Campero and W. Fillius, *ibid.* **81**, 1289 (1976).
15. T. R. McDonough and N. M. Brice, *Nature (London)* **242**, 513 (1973).
16. A. L. Broadfoot *et al.*, *Science* **212**, 206 (1981).
17. L. J. Lanzerotti, C. G. MacLennan, T. P. Armstrong, S. M. Krimigis, R. P. Lepping, N. F. Ness, *J. Geophys. Res.*, in press.
18. E. J. Smith, L. Davis, Jr., D. E. Jones, P. J. Coleman, Jr., D. S. Colburn, P. Dyal, C. P. Sonett, *ibid.* **85**, 5655 (1980).
19. M. L. Kaiser, M. D. Desch, J. W. Warwick, J. B. Pearce, *Science* **209**, 1238 (1980).
20. A. J. Dessler and V. M. Vasyliunas, *Geophys. Res. Lett.* **6**, 37 (1979).
21. M. Schulz and L. J. Lanzerotti, in *Physics and Chemistry in Space*, J. G. Roederer, Ed. (Springer-Verlag, New York, 1974), vol. 7.
22. J. H. Wolfe, J. D. Mihalov, H. R. Collard, D. D. McKibbin, L. A. Frank, D. S. Intriligator, *Science* **207**, 403 (1980).
23. We thank the Voyager Project Office, JPL, and the Planetary Programs Office, NASA Headquarters, for help and cooperation in carrying out this experiment. We thank D. P. Peletier, S. A. Gary, R. G. King, J. W. Kohl, D. E. Fort, J. T. Mueller, J. H. Crawford, R. E. Thompson, B. A. Northrop, and J. Hook at APL/JHU; E. O. Tums, J. C. Cain, R. T. Cates, R. A. Lundgren, and D. C. Brown of the University of Maryland; C. G. MacLennan of Bell Laboratories; and J. O'Donnell, S. T. Brandon, and M. Paonessa of the University of Kansas for their enthusiasm and long hours that made the LECP experiment a success. The work of E. Franzgrote and D. Griffith of JPL (among many others) was essential to the success of our investigation. We thank N. F. Ness and the MAG team for making their data available before publication, and W. H. Ip for discussions on satellite effects. The LECP program was supported at APL/JHU by NASA under Task I of contract N00024-78-C-5384 between the Johns Hopkins University and the Department of the Navy and by subcontract at the Universities of Kansas and Maryland.

9 February 1981

Energetic Charged Particles in Saturn's Magnetosphere: Voyager 1 Results

Abstract. *Voyager 1 provided the first look at Saturn's magnetotail and magnetosphere during relatively quiet interplanetary conditions. This report discusses the energetic particle populations of the outer magnetosphere of Saturn and absorption features associated with Titan and Rhea, and compares these observations with Pioneer 11 data of a year earlier. The trapped proton fluxes had soft spectra, represented by power laws $E^{-\gamma}$ in kinetic energy E , with $\gamma \sim 7$ in the outer magnetosphere and $\gamma \sim 9$ in the magnetotail. Structure associated with the magnetotail was observed as close as 10 Saturn radii (R_S) on the outbound trajectory. The proton and electron fluxes in the outer magnetosphere and in the magnetotail were variable and appeared to respond to changes in interplanetary conditions. Protons with energies ≥ 2 million electron volts had free access to the magnetosphere from interplanetary space and were not stably trapped outside $\sim 7.5 R_S$.*

Voyager 1 traversed Saturn's magnetosphere during relatively quiet interplanetary conditions. The cosmic-ray subsystem (CRS) experiment (1) extended the morphology of the outer magnetosphere, as reported by the Pioneer 11 investigators (2), to higher latitudes and significantly different interplanetary conditions and provided the first information about the magnetotail at angles $> 90^\circ$ from the Saturn-sun line. A detailed comparison of data from the two missions is important for identifying the processes that shape Saturn's magnetosphere. The Voyager 1 CRS data presented here are restricted to the outer portions of the magnetosphere [$L \geq 7.5$ (3)], where the instrument could clearly resolve electrons from protons.

Magnetospheric morphology. Counting rates of protons with energies > 0.43

MeV and 1.8 to 8 MeV are shown in Fig. 1. Also shown are corresponding normalized rates with similar energy thresholds observed by Pioneer 11 (4). Voyager 1 entered the magnetosphere three times between 23.7 and 22.9 Saturn radii (R_S) (5). Enhancements in the > 0.43 -MeV proton flux were observed at each entry. Since no similar flux enhancements were observed during the intervening passages out of the magnetosphere, it is more likely that the enhancements were the result of a transient increase in proton intensity associated with the expansion of the magnetosphere than the result of a permanent layer at the magnetopause. Thus the enhancements observed in the magnetosphere at 22.0 and 21.6 R_S (fourth and fifth peaks) may also have been due to continued radial oscillations of the magnetopause.

The > 0.43 -MeV proton flux observed by the Voyager 1 CRS experiment was more intense and peaked farther from Saturn than the > 0.55 -MeV proton flux measured by Pioneer 11 (Fig. 1). These differences were at least partly due to the different threshold energies and latitudes of the spacecraft's trajectories, although the Voyager data suggest that the flux decrease near $L = 9$ may be attributable to absorption by Rhea.

Within the magnetosphere the proton differential energy spectra $j(E)$ (insets in Fig. 1) are well represented by the sum of two components

$$j(E) = K_1 E^{-\gamma} + \frac{K_2}{\sqrt{E}} \exp(-\sqrt{E/E_0})$$

where E is the proton kinetic energy, K_1 and K_2 are constants, γ is the power law index, and E_0 is the characteristic energy corresponding to the e -folding momentum. This two-component spectrum suggests two different sources for the protons. The exponential component was similar to the pre-encounter interplanetary proton spectrum and remained almost unchanged into the outer magnetosphere and tail regions (Fig. 1), while the power law component was of magnetospheric origin with $\gamma \sim 7$ on the inbound pass ($L > 12$), a value within 1 of those observed by Pioneer 11 (4).

At energies above 1.8 MeV, where the magnetospheric component was negligible, the proton flux observed by Voyager

1 was constant from interplanetary space into $L \sim 7.5$. A high-energy component was also observed both inside and outside the magnetosphere by Pioneer 11 (4), but it was more intense by over an order of magnitude and corresponded to the higher interplanetary flux at the time. These observations provide strong evidence that interplanetary protons above 1.8 MeV had free access to Saturn's magnetosphere—at rigidities well below the dipole Störmer cutoff value—via the magnetotail or other field distortions (4) and thus that protons of energies ≥ 2 MeV were not stably trapped outside $L \sim 7.5$.

The radial dependences of the electron intensities (Fig. 2) were similar to those measured by Pioneer 11 at comparable energies (4), except that at energies > 0.6 MeV on the outbound pass the Voyager 1 electron flux remained nearly constant from $L \sim 7$ to 9. Outbound at $L \sim 10$, a rapid decrease in the electron flux and an accompanying decrease in the > 0.43 -MeV proton flux signaled a transition, perhaps from the stable trapping region to a quasi-stable one. Beyond $L \sim 10$ the magnetic field direction indicated the onset of the magnetotail (5), and between $L = 10$ and $L = 25$ the low-energy electron and proton fluxes both showed large time-dependent variations. The rapid flux increase at $L \sim 14$ may have been the result of a change in interplanetary conditions. Plasma mea-

surements on Voyager 2, when extrapolated to the position of Saturn, indicate that the solar wind pressure should have doubled while Voyager 1 moved from $L = 14$ to 26 (6). Minima in the fluxes of both protons and electrons at $L = 17$ to 20 show a correlation with Titan's orbit, which may be coincidental. The proton spectrum of this tail population was extremely soft, with $\gamma = 9$ to 10.

Voyager 1 traversed the magnetotail between 25 and $\sim 45 R_S$ (Fig. 3) at a latitude $> 20^\circ$ and a local time of ~ 0300 hours. An appreciable flux of electrons (0.15 to 0.4 MeV) was observed over most of this period (Fig. 3), while the proton flux had dropped to near-interplanetary values. The relatively intense electron flux observed at these latitudes demonstrates that the electrons were not confined to an equatorial current sheet. This contrasts with the Jovian magnetotail and may result from a less distended field configuration. Tailward-streaming bursts of > 0.43 -MeV protons were observed sporadically throughout the region.

Saturn's magnetotail is probably a key to the properties of the outer magnetosphere. In Saturn's magnetotail, as at Earth and Jupiter, changes in the tail configuration induced by interplanetary disturbances may lead to the acceleration of both ions and electrons to several hundred kiloelectron volts. The Titan hydrogen torus (7) is a likely source of

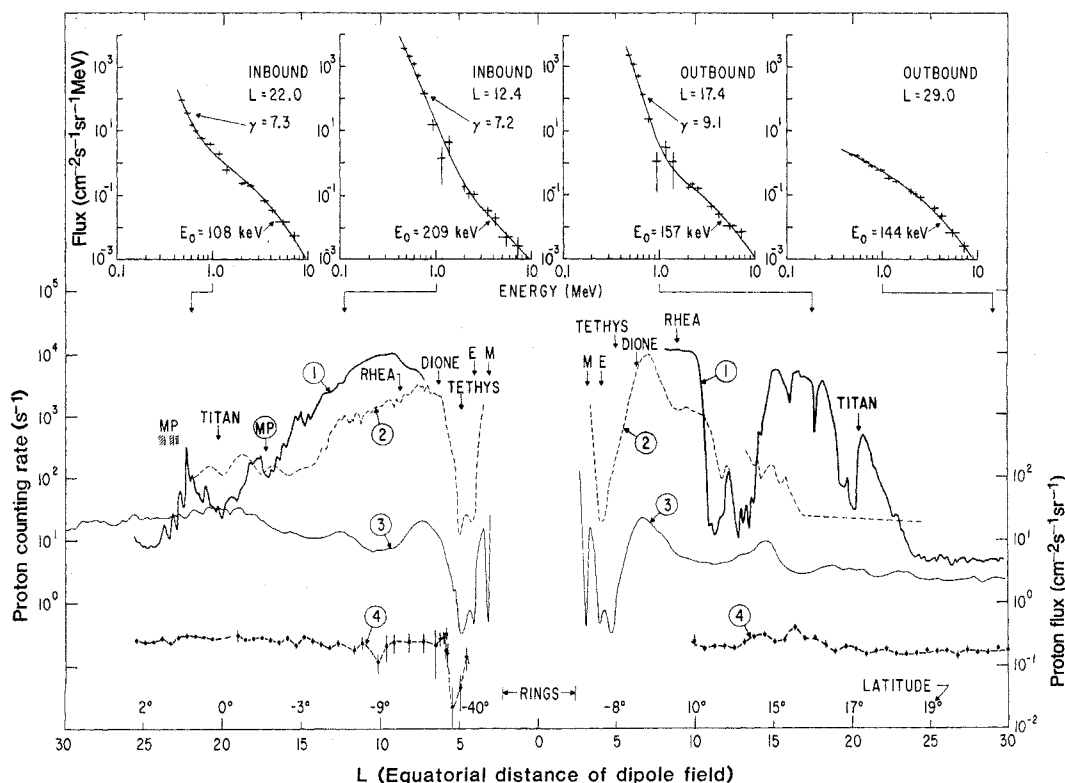


Fig. 1. Proton intensities versus L and proton spectra in Saturn's magnetosphere. Curve 1 gives the counting rate of > 0.43 -MeV protons from Voyager 1 and curve 2 gives a similar rate (> 0.55 MeV) as obtained by Pioneer 11, normalized to the geometric factor of the Voyager instrument. Curve 3 shows the Pioneer 11 1.6- to 5-MeV proton flux and curve 4 shows the Voyager 1 flux of 1.8- to 8-MeV protons (right-hand scale). On the inbound pass, the magnetosheath extends to $L \sim 24$ and is indicated by shaded areas near the magnetopause (MP) crossings. Voyager 1 latitudes are shown above the distance scale. Pioneer 11 remained within 5° of the equator. Proton spectra are shown in the insets. The power law index γ for the low-energy end is given as well as the characteristic energy E_0 for the high-energy end. Pre-encounter spectra were almost indistinguishable from the tail spectrum at $L = 29$.

these ions, which are further energized as they diffuse inward through the conservation of the first and second adiabatic invariants (8). This process explains why the proton-to-alpha ratio in Saturn's magnetosphere (4) is larger than that in the interplanetary medium.

Energetic charged particle absorption by Rhea and Titan. Voyager 1 crossed the orbits of Rhea and Titan at longitudes close to those of the moons. There were localized decreases in the charged particle intensity because of absorption of the trapped radiation by the moons. Figure 4 shows the absorption signature observed in five independent counting rates just outside $L = 8.5$, significantly inside the dipole L shell ($L = 8.8$) of Rhea. Despite the apparent discrepancy in position, this feature was almost certainly due to Rhea, since it was the only signature observed in this region. The widths at half-minimum of the absorption feature observed by the low-energy telescope (LET) detectors were ~ 3000 to 4000 km; this is what would be expected for absorption by Rhea [radius, 765 km (9)] of 0.5 -MeV protons, which had gyroradii of ~ 3500 km in this region.

Over the time period shown in Fig. 4, Voyager 1 was $\sim 1 R_S$ north and $\sim 4^\circ$ east of Rhea; thus it took the magnetospheric plasma ~ 7 minutes to corotate from Rhea to Voyager 1. Since protons drift to the east, in the same direction as Saturn's rotation, protons observed at this time had passed Rhea less than 7 minutes earlier (~ 3 minutes for 0.5 -MeV protons). Electrons drift in the opposite direction, however, and thus must have passed Rhea more than 7 minutes earlier. In a dipole field, electrons with energies > 0.58 MeV (at 60° pitch angle) have drift velocities greater than Rhea's orbital velocity relative to the magnetospheric plasma; thus the absorption signature of these electrons would be on the other side of Rhea. Therefore the absorption feature observed in the electron telescope (TET) counting rate must have been due to electrons with energies just below the nominal 0.60 -MeV threshold.

Given that this absorption feature was due to Rhea, the position of this feature may be used to infer the magnitude of the nondipole deformations of Saturn's magnetic field near $9 R_S$ at a local time of 0200 hours. Since charged particles closely follow magnetic field lines during their latitudinal bounce motion, the Rhea flux absorption feature provides a tracer of the field lines that pass the position of Rhea in the equatorial plane. The distortion of the field which is inferred by this method is illustrated in Fig. 5. The labeled points along the Voyager 1 trajec-

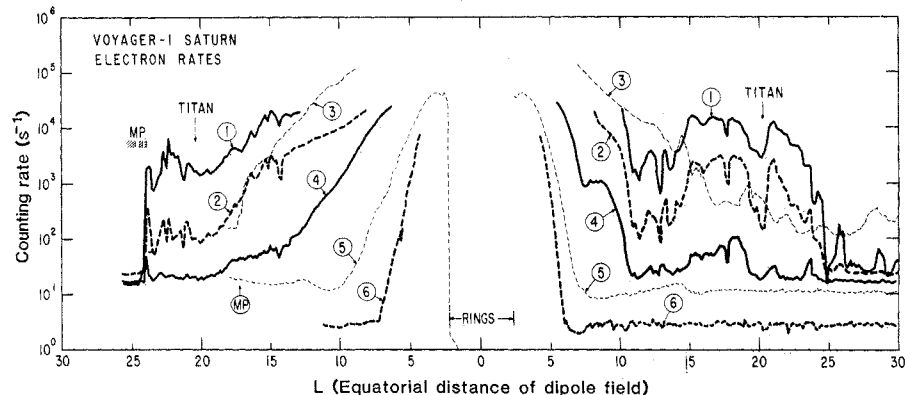


Fig. 2. Electron intensities versus L in Saturn's magnetosphere. The Voyager 1 data in curves 1, 2, 4, and 6 correspond to electron energies of 0.15 to 0.4 MeV, > 0.35 MeV, > 0.60 MeV, and > 2.6 MeV, respectively. Curves 3 and 5 give Pioneer 11 rates for energies above 0.25 and 2.0 MeV, respectively, normalized to the geometric factors of the Voyager instrument. Near the magnetopause the magnetosheath is indicated by the shaded area.

Fig. 3. Voyager 1 electron and proton intensities in the magnetotail at northern latitudes between 20° and 23° versus distance from Saturn. Shaded areas indicate periods when the spacecraft was in the magnetosheath.

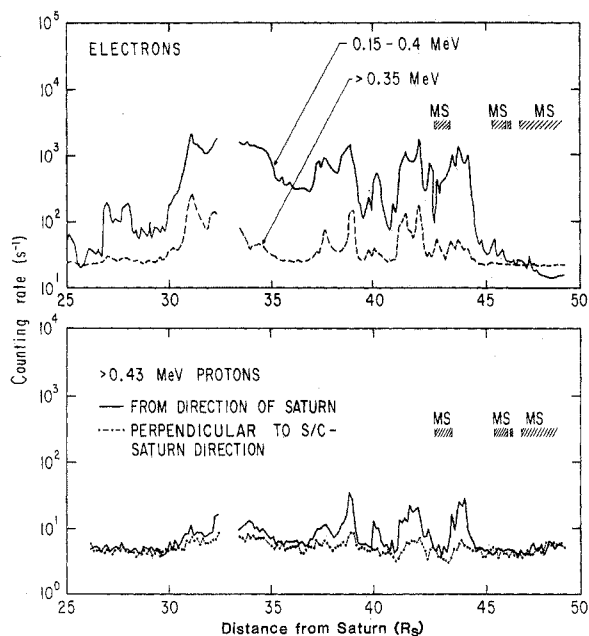


Fig. 4. Counting rates of five CRS detectors on Voyager 1 in the vicinity of Rhea along the outbound pass versus SCET. LET A, LET B, and LET D label counting rates of essentially identical detectors that respond to protons with energies > 0.43 MeV and have a low electron detection efficiency. The differences between LET A, B, and D counting rates are roughly consistent with the expected unidirectional anisotropy due to Saturn's rotation. HET 2 and TET label counting rates of detectors with nominal threshold energies for detecting electrons of 0.35 and 0.60 MeV, respectively.

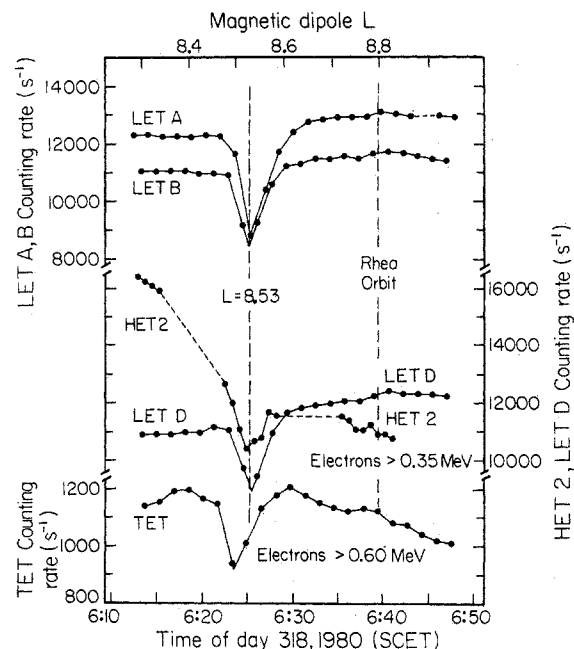
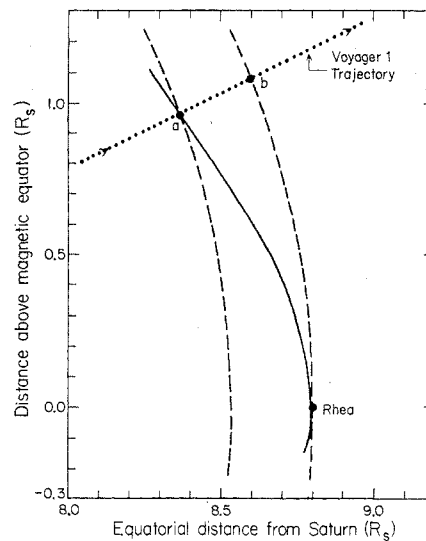


Fig. 5. Voyager 1 trajectory near Rhea, distortion of the magnetic field inferred from the Rhea absorption feature (solid line), and the shapes of dipole field lines in this region (dashed lines).

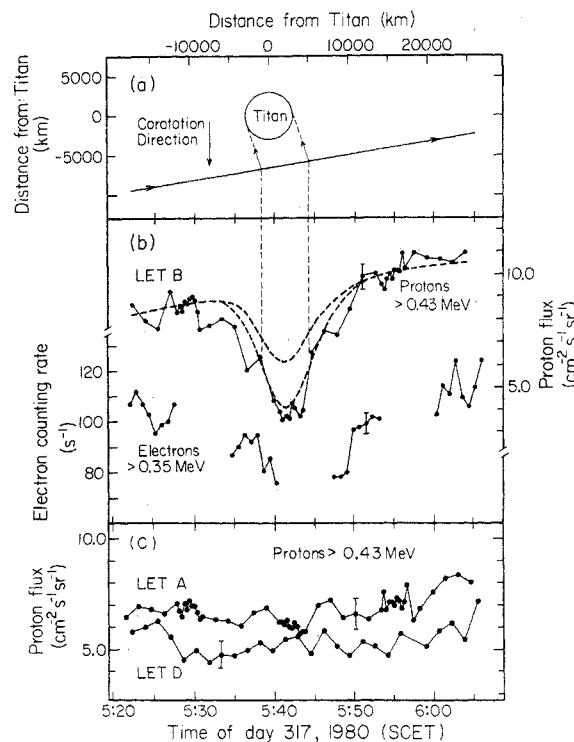
tory indicate the observed positions of the Rhea absorption feature (Fig. 5, a) and the position expected on the basis of a magnetic dipole model (Fig. 5, b). Dashed curves show the shapes of two dipole field lines and the solid line represents the inferred distorted field line. The magnitude and direction of this deformation are consistent with the amount of nondipolar distortion of the field measured by the Voyager 1 magnetometer at this time (5). Such a distortion could be produced by an equatorial current in Saturn's magnetosphere or by a magnetotail neutral sheet current.

Since protons mirroring off the equatorial plane have a significant probability of missing Rhea, the depth of the absorption signature depends on position and pitch angle. The ~ 3 -minute separation between Voyager 1 and Rhea was about one bounce period for 0.5-MeV protons. Thus Voyager 1 passed behind Rhea where the 0.5-MeV proton flux was locally most heavily absorbed. The distance behind Rhea at which the absorption is most complete depends on pitch angle through the pitch angle dependence of the bounce and drift periods.



In contrast to the situation at Rhea, the Voyager 1 close approach to Titan provided the opportunity to observe charged particle absorption at distances smaller than the local 0.5-MeV proton gyroradius [$\sim 20,000$ km in a 5-nT magnetic field (5)]. The large decrease in the LET B proton flux (Fig. 6b) centered at 05:42 spacecraft event time (SCET) has a natural interpretation as a "shadow image" of Titan, formed as Titan intercepted the field of view of the LET B detector. The > 0.43 -MeV proton fluxes measured by each of two other detectors, which did not view Titan (Fig. 6c), show

Fig. 6. (a) Voyager 1 trajectory in Titan-fixed coordinates, projected onto Saturn's equatorial plane. The distance scale is chosen such that the bottom time scale also labels SCET along the trajectory. (b) Flux of > 0.43 -MeV protons measured by the LET B detector, which looked toward Titan in the direction of the arrows shown along the trajectory trace in the upper panel, versus SCET, and the counting rate of electrons > 0.35 MeV versus SCET. Samples of the electron counting rate were obtained in alternate 6.4-minute intervals. Vertical dashed lines define the interval when Titan covered the center of the LET B field of view. Heavy dashed curves drawn over the LET proton flux show the calculated Titan absorption signature in LET B for an isotropic proton flux, assuming absorption radii of 2860 km (upper curve) and 3800 km (lower curve). (c) Fluxes of > 0.43 -MeV protons, as measured by the LET A and LET D detectors, versus SCET.



no statistically significant absorption. Each of these detectors was oriented $\sim 80^\circ$ from the spacecraft-Titan direction and neither was pointing within 35° of the equatorial plane. Thus no proton shadow due to Titan would have been expected in these detectors. In addition, Titan's effect on the observed electron flux should be different from its effect on the protons because of the smaller electron gyroradius (~ 460 km at 0.35 MeV). However, gaps in the electron counting rate data (Fig. 6b) do not permit detailed analysis.

The dashed curves overlaid on the LET B proton flux show the absorption profile due to the shadow of Titan on an otherwise isotropic proton flux. The upper curve was calculated by assuming a radius for the absorber of 2860 km, the visible radius of Titan (10), while the lower curve, which provides a better fit to the data, was obtained by assuming a radius of 3800 km—nearer the top of Titan's atmosphere (11). Since the model used to calculate the absorption profile assumed an isotropic proton flux, an anisotropic flux with a maximum near 90° pitch angles, as suggested by our data, will result in some overestimate of Titan's effective absorption radius.

R. E. VOGT

D. L. CHENETTE, A. C. CUMMINGS
T. L. GARRARD, E. C. STONE

California Institute of Technology,
Pasadena 91125

A. W. SCHARDT, J. H. TRAINOR
N. LAL, F. B. McDONALD

NASA Goddard Space Flight Center,
Greenbelt, Maryland 20771

References and Notes

1. E. C. Stone, R. E. Vogt, F. B. McDonald, B. J. Teegarden, J. H. Trainor, J. R. Jokipii, W. R. Webber, *Space Sci. Rev.* **21**, 355 (1977).
2. Collections of earlier results from the Pioneer 11 encounter with Saturn are to be found in the "Saturn" issues of *Science* **207** (No. 4429) (1980) and *J. Geophys. Res.* **85** (No. A11) (1980).
3. We define L as $R/\cos^2\lambda$, where R is radial distance in Saturn radii ($1 R_S = 60,000$ km) and λ is latitude.
4. F. B. McDonald, A. W. Schardt, J. H. Trainor, *J. Geophys. Res.* **85**, 5813 (1980).
5. N. F. Ness *et al.*, *Science* **212**, 211 (1981).
6. P. Gazis and J. D. Sullivan, personal communication.
7. A. L. Broadfoot *et al.*, *Science* **212**, 206 (1981).
8. J. G. Roederer, *Dynamics of Geomagnetically Trapped Radiation* (Springer-Verlag, Berlin, 1970), pp. 19, 50.
9. B. A. Smith *et al.*, *Science* **212**, 163 (1981).
10. P. H. Smith, *J. Geophys. Res.* **85**, 5943 (1980).
11. The atmospheric pressure and the ~ 45 -km scale height inferred by Broadfoot *et al.* (7) at 3500 km from the center of Titan yield a density about ten times that required to stop a 0.5-MeV proton grazing at that altitude.
12. We thank the Voyager project members and the enthusiastic staff of our laboratories at Caltech and Goddard Space Flight Center for their splendid support. Special thanks go to W. Alt-house, N. Gehrels, and I. Matus (Caltech), W. Davis, H. Domchick, and D. Stilwell (Goddard), and E. Franzgrote (Jet Propulsion Laboratory). Supported by NASA under NAS7-100 and NGR 05-002-160.

9 February 1981